Title

Human defensin-inspired discovery of peptidomimetic antibiotics.

Permalink

https://escholarship.org/uc/item/8h88378h

Journal

Proceedings of the National Academy of Sciences of USA, 119(10)

Authors

Luo, Gan

Zhang, Jue

Wang, HanBin

et al.

Publication Date

2022-03-08

DOI

10.1073/pnas.2117283119

Peer reviewed

Human defensin-inspired discovery of peptidomimetic antibiotics

Gan Luo[a,1], Jue Zhang[a,1] (ID), HanBin Wang[a,1], YaQi Sun[a], BaoLi Cheng[a], ZhiPeng Xu[a], Yan Zhang[b], Hui Li[a], WuYuan Lu[c,2], Elizabeta Nemeth[d,2] (ID), Tomas Ganz[d,2] (ID), and XiangMing Fang[a,2] (ID)

[a]Department of Anesthesiology and Intensive Care, The First Affiliated Hospital, School of Medicine, Zhejiang University, Hangzhou 310003, China; [b]National Clinical Research Center for Child Health, Children's Hospital, School of Medicine, Zhejiang University, Hangzhou 310052, China; [c]Key Laboratory of Medical Molecular Virology, School of Basic Medical Sciences, Fudan University, Shanghai 200032, China; and [d]Department of Medicine, David Geffen School of Medicine, University of California, Los Angeles, CA 90095

Antibiotics with multiple mechanisms of action and broad-spectrum are urgently required to combat the growing health threat posed by resistant pathogenic microorganisms. Combining computational and medicinal chemistry tools, we used the structure of human α-defensin 5 (HD5) to design a class of peptidomimetic antibiotics with improved activity against both gram-negative and gram-positive bacteria. The most promising lead, compound 10, showed potent killing of multiple drug-resistant gram-negative bacteria isolated from patients. Compound 10 exhibited a multiplex mechanism of action through targeting membrane components—outer membrane protein A and lipopolysaccharide, as well as a potential intracellular target—70S ribosome, thus causing membrane perturbation and inhibition of protein synthesis. In vivo efficacy, stability, and safety of compound 10 were also validated. This human defensin-inspired synthetic peptidomimetic could help solve the serious problem of drug resistance to conventional antibiotics.

defensins | peptidomimetic antibiotics | antimicrobial resistance | infections

Antimicrobial resistance is a serious threat to human health. By 2050, an estimated 10 million people are projected to die annually of infections complicated by antimicrobial resistance (1–3). Novel antimicrobials with de novo structures, broad-spectrum activity, and multimodal mechanisms are urgently needed (4). However, exhaustion of traditional antimicrobial resources has seriously challenged conventional screening approaches because of the high frequency of rediscovering known compounds, which thus have slowed the development of alternative antibiotics that possess de novo structural scaffolds, novel mechanisms of action (MoA), and extended antimicrobial spectra (5).

The human body is a valuable chemical resource that harbors host-protective cationic antimicrobial peptides (CAMPs), which have been investigated as a class of promising templates for antibiotic development (6). However, natural CAMPs are often unsuitable for direct clinical translation for various reasons, including suboptimal antimicrobial activity, poor pharmacokinetic properties, low proteolytic stability, and high costs for production (7, 8). To improve the pharmacological viability of natural CAMPs, a number of peptidomimetic chemistries have been successfully developed, among which are "foldamers" of unnatural amino acids mimicking the structure and function of naturally occurring CAMPs (7–12), small molecule-based peptidomimetics, such as the flavonoid scaffold decorated with cationic residues/moieties (13–15), and protegrin-derived β-hairpin peptidomimetics (5, 16).

Our group has exploited a different peptidomimetic approach using human endogenous enteric defensins. Human α-defensin 5 (HD5), a natural CAMP secreted by intestinal Paneth cells (17, 18), is bactericidal to both gram-negative and gram-positive bacteria through a well-established MoA of membrane perturbation (19). The development of HD5 is hampered by unfavorable

pharmacological properties along three major axes: 1) insufficient activity to meet requirement of clinical therapeutics; 2) inhibition of activity by serum and physiological ionic microenvironment; and 3) a relatively large size and complex structure that challenges chemical modification and synthesis. To date, no approach has resolved these critical issues ideally. From our perspective, overcoming these challenges necessitates simplification of full-length HD5 into a simple mini-HD5 that allows highly accessible synthesis and subsequent peptidomimetic efforts to improve drug-like properties, including bactericidal activity, physicochemical/biological stability, and cost of synthesis. Guided by these concepts, we set out to simplify and redesign HD5 into an antimicrobial compound that overcomes the shortcomings of the parent defensin HD5.

Here, we successfully redesigned HD5 as a class of peptidomimetic antibiotics by combining computational and medicinal chemistry approaches. A structure–activity relationship (SAR) study identified peptidomimetic antibiotic **10** as the "best-in-class" candidate that showed a synthesis-friendly linear structure, powerful bactericidal action, and favorable therapeutic index. Further efforts found **10** interrupted the membrane integrity and preserved the membrane activity of its parent defensin HD5 through targeting outer membrane protein A (OmpA) and lipopolysaccharide (LPS) on the surface of gram-negative outer membrane (OM). In addition, we also found that **10** targeted bacterial 70S ribosomes. Finally, in vivo efficacy and toxicity were validated in infected and healthy mice, respectively. The in vivo stability was assessed through

---

Significance

We report the development of peptidomimetic antibiotics derived from a natural antimicrobial peptide, human α-defensin 5. By engaging multiple bacterial targets, the lead compound is efficacious in vitro and in vivo against bacteria with highly inducible antibiotic resistance, promising a useful therapeutic agent for the treatment of infections caused by antibiotic-resistant bacteria.

pharmacokinetics. The flow-process pipeline for this rational design of HD5 is summarized in Fig. 1*A*.

Materials and Methods

All peptidomimetic chemicals were synthesized by solid-phase peptide synthesis and purchased from Shanghai Apeptide. Computational studies and biological assays, including molecular docking, molecular dynamics simulations, bacterial culture, bactericidal assays, and cell viability assays, were performed by using standard approaches, with all methods detailed in *SI Appendix*. Animal studies were approved and guided by the Animal Advisory Committee at Zhejiang University.

Results

Structure-Guided Identification of Pharmacophores and Lead Compounds.

Our pipeline to design defensin-inspired antibiotics started with the identification of pharmacophores that form the HD5 interactive biointerface with multiple bacterial targets, including bacterial envelopes, LPS, OmpA (e.g., *Acinetobacter baumannii*), and lipid II (e.g., *Staphylococcus aureus*) (Fig. 1*A* and *SI Appendix*, Fig. S1) (17, 20–24). Previous research has demonstrated that residues A^1, T^2, R^6, R^{13}, and R^{32} are crucial for HD5 to adsorb to the LPS-containing OM, and basic residues (R^6, R^9, R^{13}, R^{25}, R^{28}) for HD5 to electrostatically interact with the inner membrane (IM) (25, 26). To fully map out pharmacophore biointerfaces, we modeled HD5 interactions with *A. baumannii* OmpA and *S. aureus* lipid II using computational biology approaches (*SI Appendix*, Figs. S2 and S3). After molecular dynamic analysis, the contact residues were conclusively identified (*SI Appendix, SI Materials and Methods*, and Figs. S2 and S3, and Movie S1). Our structure-guided analysis in combination with the previous findings by others identified motifs T^2-C^3-Y^4-C^5-R^6-T^7-G^8 in the β1 strand and R^{25}-L^{26}-Y^{27}-R^{28} in the β3 strand as potential pharmacophores responsible for the antimicrobial activity of HD5 (Fig. 1*B*). We synthesized lead peptides **1** and **2** corresponding to the two identified pharmacophores (Fig. 1*C*), and both peptides exhibited bactericidal activity (Fig. 1*D*). Lead peptide **1** exhibited
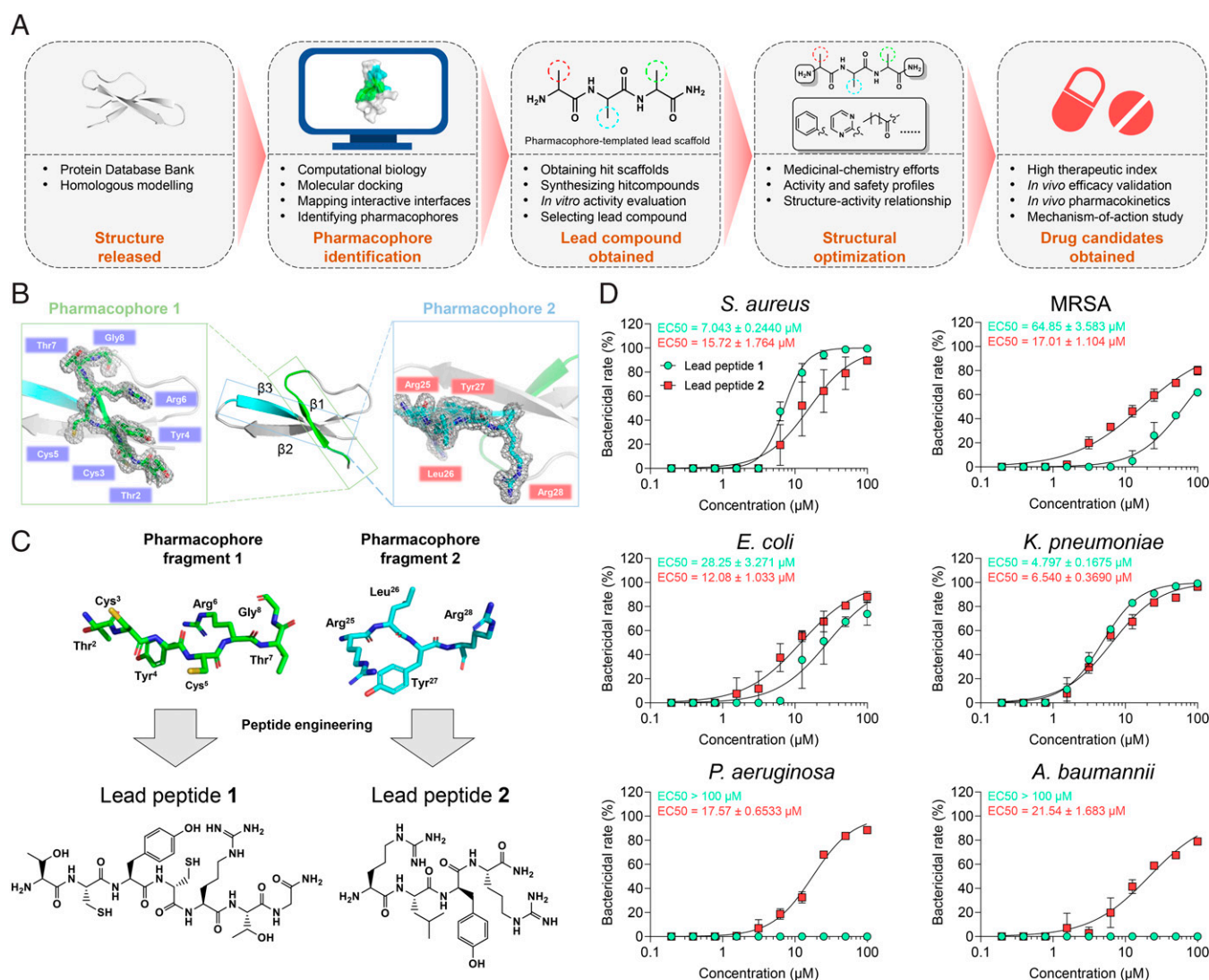
Fig. 1. Structure-guided discovery of pharmacophores and lead scaffolds in HD5. (*A*) Schematic illustration of the pipeline for discovering/designing HD5-inspired peptidomimetic antibiotics. (*B*) Cartoon models of HD5 highlighting its potential pharmacophore motifs. Pharmacophores 1 and 2 are colored green and cyan, respectively. Zoomed views are presented to indicate the biointerfaces and structures of pharmacophores in which residues are labeled. The $2F_o$–F_c electron density maps are shown around the pharmacophores (gray mesh), and electron density map information was retrieved from the Protein Data Bank (http://www.rcsb.org/pdb/explore/explore.do?structureId=1ZMP). (*C*) Design and synthesis of lead peptides based on the pharmacophore templates. (*D*) In vitro bactericidal activity of lead peptides against members of ESKAPE pathogens. Data are presented as mean ± SD. The EC_{50} values of the two lead peptides are indicated for each pathogen, which are fitted by using a four-parameter dose–response model. The experiment was performed in triplicate.

considerable activity against *S. aureus* in vitro (EC$_{50}$ ~7.043 ± 0.2440 µM) but 10-fold higher EC$_{50}$ against methicillin *S. aureas* (MRSA), whereas lead peptide **2** had comparable activity against both pathogens (EC$_{50}$ ~15.72 ± 1.764 µM and 17.01 ± 1.104 µM). Lead peptide **2** was more active than **1** against *Escherichia coli* (EC$_{50}$ ~12.08 ± 1.033 µM vs. 28.25 ± 3.271 µM), but both exhibited similar activity against *Klebsiella pneumoniae*. Notably, lead peptide **1** did not show any bactericidal activity against *Pseudomonas aeruginosa* and *A. baumannii* within the range of concentrations used (EC$_{50}$ > 100 µM), while lead peptide **2** demonstrated concentration-dependent killing of the two pathogens, with EC$_{50}$ values of ~17.57 ± 0.6533 µM and ~21.54 ± 1.683 µM, respectively. Since the two lead peptides were less effective in bacterial killing than their parent defensin HD5 (*SI Appendix,* Fig. S4), the use of medicinal chemistry tools was warranted for functional improvement. Considering its bactericidal effect and broad-spectrum activity, we selected peptide **2** as the lead compound for structural optimization.

Peptidomimetic Chemistry-Guided Structural Optimization and SAR. The tetra-peptide backbone R^{25}-L^{26}-Y^{27}-R^{28} of lead compound **2** consists of positively charged, hydrophobic, and aromatic groups that could support access to bacterial envelopes. We maintained this core structure in the next round of design as it likely contributed to the superior bactericidal activity of lead compound **2**. The R$_1$/R$_2$ moieties located at the N and C termini were used for chemical functionalization and subsequent structural optimization (Fig. 2*A*). We employed three peptidomimetic strategies, including appending potent electron-donating or hydrophobic moieties (e.g., long alkyl groups), substitution by aromatic groups, and replacement by heteroaromatic groups (Fig. 2*A*), which generated a family of peptidomimetic antibiotics (identifier **3∼10**) (Fig. 2*B*).

Improved bactericidal activity was achieved via an N-terminal cap of a long alkyl group, including palmityl, lauryl, or myristyl, which generated antibiotics **3**, **4**, and **5**, respectively. All three peptidomimetic antibiotics had significantly stronger bactericidal activity than **2** (Fig. 1*D* and *SI Appendix,* Fig. S5). Notably, **3** is at least 200-fold more potent than HD5 against *K. pneumoniae* (EC$_{50}$ ~0.2298 ± 0.01212 µM vs. 26.43 ± 2.415 µM) and *P. aeruginosa* (EC$_{50}$ ~ < 0.195 µM vs. 12.53 ± 1.507 µM). Interestingly, shortening the alkyl group in **3** to a lauryl group, resulting in compound **4** (Fig. 2*B*), increased the compound's performance against gram-positive pathogens (*S. aureus* and MRSA); however, this modification attenuated the activity against gram-negative pathogens, though with the benefit of decreasing its cytotoxicity to mammalian cells (*SI Appendix,* Fig. S6 *A* and *B*). Replacing palmityl with myristyl yielded **5**, which improved the activity against *S. aureus* and MRSA, while maintaining the activity against gram-negative ESKAPE members (*Enterococcus faecium, S. aureus, K. pneumoniae, A. baumannii, P. aeruginosa, Enterobacter* spp.), including *E. coli, K. pneumoniae,* and *A. baumannii*. Antibiotic **5** also showed lower cytotoxicity than **3** and lower concentration for killing 99% bacteria (LC99) for these six bacteria than did **3**, **4**, and HD5 (*SI Appendix,* Figs. S6*C* and S11).

Replacing the long alkyl chain with 2-(4-(*tert*-butyl)phenyl)-4-methylpyrimidine-5-carboxylic acid, a heteroaromatic group previously used to replace the lipopeptide tail in arylomycin optimization (27), led to a decrease in bactericidal activity (*SI Appendix,* Fig. S7*A*). Nevertheless, the resultant compound **6** still exhibited stronger activity than **2** (Fig. 1*D* and *SI Appendix,* Fig. S7*A*), especially against *S. aureus* and *E. coli*, with ~30-fold enhancement of activity. Importantly, compound **6** did not show any cytotoxicity to the three mammalian cell lines at the range of concentrations tested, suggesting a favorable safety profile (*SI Appendix,* Fig. S8*A*). To further improve bactericidal activity, we appended the heteroaromatic group to the C terminus of **5** and generated compound **7**, which showed systematic
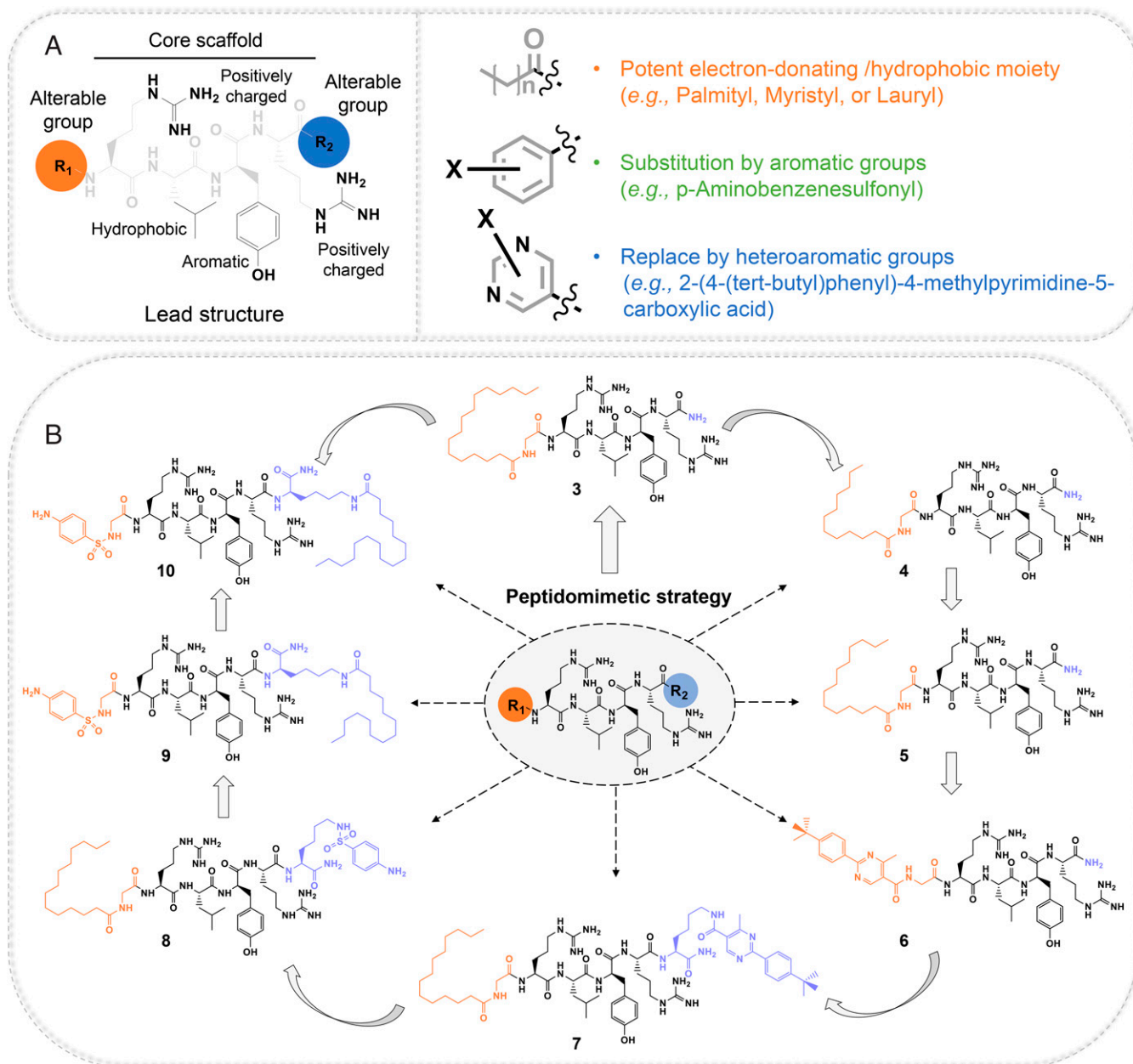
decreases in EC$_{50}$ compared with HD5 and compounds **2** and **5** (Fig. 1*D* and *SI Appendix,* Figs. S4, S5*C*, and S7*B*). However, **7** exerted higher cytotoxicity to the three mammalian cells than all of the above compounds (*SI Appendix,* Fig. S8*B*).

To overcome the safety shortcomings observed with **7**, we tested aromatic substitutions. Replacing the heteroaromatic group with p-aminobenzenesulfonyl dramatically alleviated the cytotoxicity of **7** (*SI Appendix,* Fig. S9*A*). However, the resulting compound **8** showed at least a threefold decrease in bactericidal activity against MRSA, *E. coli, K. pneumoniae,* and *P. aeruginosa*, while comparable with compound **7** against *S. aureus* and *A. baumannii* (*SI Appendix,* Fig. S10*A*). Swapping the N- and C-terminal modifications of **8** resulted in **9**, which exhibited a favorable safety profile with peritoneal macrophages and hepatocyte BNL CL.2 cell line, but an eightfold enhancement in cytotoxicity to the fibroblast 3T3 cell line (*SI Appendix,* Fig. S9*B*). The antimicrobial activity of **9** decreased substantially compared with that of **8** (*SI Appendix,* Fig. S10*B*). Unexpectedly, substituting the myristyl group of **9** with palmityl yielded a structural analog termed **10** that showed the highest activity against ESKAPE pathogens (*SI Appendix,* Fig. S10*C*) with relatively low cytotoxicity and the lowest LC99 values among other family members (*SI Appendix,* Figs. S9*C* and S11). Considering its potency and a wide therapeutic window (EC$_{50}$ < 0.50 µM and CC50 > 20 µM, safety index > 40) (Fig. 3*A*), antibiotic **10** was selected as the "best-in-class" antibiotic candidate for in-depth investigation.

Peptidomimetic 10 Is an Effective Broad-Spectrum Antibiotic against High-Risk Clinical Isolates. SAR-directed drug screening clearly indicated **10** is the most powerful one among these defensin-inspired peptidomimetics against ESKAPE pathogens with favorable therapeutic index (Fig. 3*A*). To further assess its clinical potential, we tested the bactericidal activity of the compound against clinically isolated pathogens with high risk and lethality (Fig. 3*B*). Both **10** and its homologous compound **5** exhibited potent killing of clinical isolated *Listeria monocytogenes, S. aureus,* and *Staphylococcus epidermidis*, in which **10** shows significantly superior activity, suggesting it is also best-in-class in clinical isolates. Nevertheless, compound **10** did not exhibit significant advantages relative to Imipenem Cilastatin in combatting the three isolates, especially for *S. aureus* and *S. epidermidis*. For *Salmonella typhimurium* and other clinically isolated drug-resistant bacteria, including carbapenem-resistant (CR) *K. pneumoniae*, CR-*P. aeruginosa*, pandrug-resistant (PDR) *Providencia rettgeri* and PDR-*A. baumannii*, Imipenem Cilastatin showed very limited activity, while **10** still maintained high-performance killing comparable to the last-resort antibiotic polymyxin B (PMB) (Fig. 3*B* and *SI Appendix,* Fig. S12). These results all demonstrated that **10** was a promising candidate for further development.

Peptidomimetic Antibiotic 10 Retains the Membrane Activity of Defensin. Given the broad-spectrum and potent activity against gram-negative bacteria that are difficult-to-treat in clinic, we sought to uncover the MoA of **10** by using bacterial model of *E. coli* ATCC25922. Membrane perturbation represents the most common mechanism against gram-negative bacteria for defensins. Thus, we examined if **10** retains the membrane activity of its parent defensin HD5 to penetrate the membrane barrier of gram-negative bacteria. As expected, addition of **10** to *E. coli* indeed resulted in irregularly shaped holes in the bacterial membrane barrier, similar to those generated by HD5 and PMB (a membrane-activity lipopeptide), while *E. coli* cells treated by kanamycin (a nonmembrane-activity antibiotic) preserved integral membrane architecture (Fig. 4*A*). Fluorescent probe 1-*N*-phenylnaphtylamine (NPN) assay indicated that treatment of **10**, HD5, or PMB increased the permeability of

Luo et al.
Human defensin-inspired discovery of peptidomimetic antibiotics

PNAS | 3 of 11
https://doi.org/10.1073/pnas.2117283119

Fig. 2. Structural optimization of the lead scaffold by peptidomimetic chemistry. (*A*) Proposed peptidomimetic-chemistry pipeline for structurally reprogramming the parent scaffold of the lead compound. (*B*) Design cycle and chemical structures of a new class of peptidomimetic antibiotics generated from the peptidomimetic strategy.

bacterial OM in a dose-dependent manner, whereas kanamycin did not (Fig. 4 *B–E*). These findings all indicated that **10** retains the membrane activity of its parent defensin HD5.

Peptidomimetic Antibiotic 10 Exerts Membrane Activity by Interacting with Surface Targets: OmpA and LPS. To further elucidate the molecular targets of **10** responsible for the membrane perturbation, a transcriptomic assay was performed to reveal the alterations of *E. coli* in response to **10**. Results demonstrated that the transcriptome alterations included multiple envelope stress pathway-related genes, indicating the disruption of envelope homeostasis (Fig. 5*A*) (28). Intriguingly, we found the expression of genes related to OM proteins (OMPs) and LPS pathway was also altered significantly (Fig. 5*B*), corresponding to the surface targets of HD5: OmpA and LPS. We initially focused

on OmpA, the major OMP of *E. coli* contributing to maintenance of OM integrity (29). Full-length OmpA comprises two independent folded structures including N-terminal β-barrel domain and C-terminal periplasmic domain (30). To assess the possibility of OmpA as one of membrane targets of **10**, we respectively expressed the two domains of *E. coli* OmpA in a prokaryotic expression system. Adding purified OmpA β-barrel domain significantly antagonized the bactericidal activity of low-dosage **10** in a concentration-dependent manner (Fig. 5*C* and *SI Appendix*, Fig. S13 *A and B*). In contrast, addition of OmpA periplasmic domain failed to affect **10**'s activity (Fig. 5*D* and *SI Appendix*, Fig. S13 *C and D*). More importantly, surface plasmon resonance (SPR) assays proved that **10** could effectively bind to OmpA β-barrel domain with a high affinity (K_D ~96 nM), similar to its parent defensin HD5 (K_D ~201 nM)
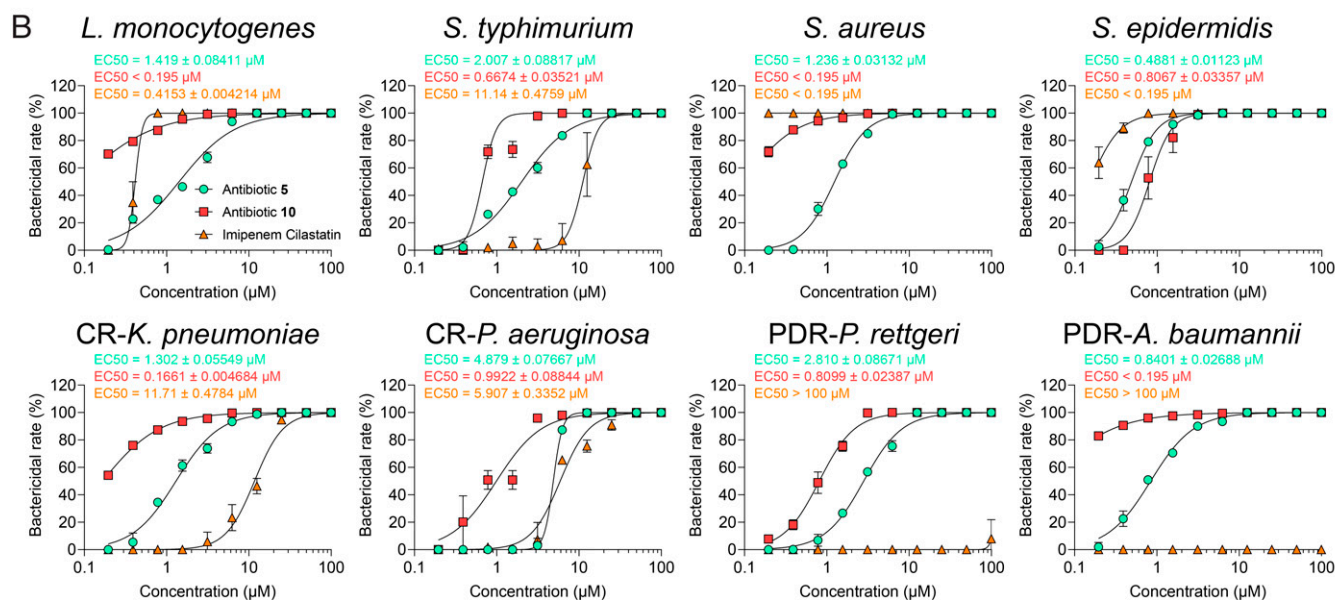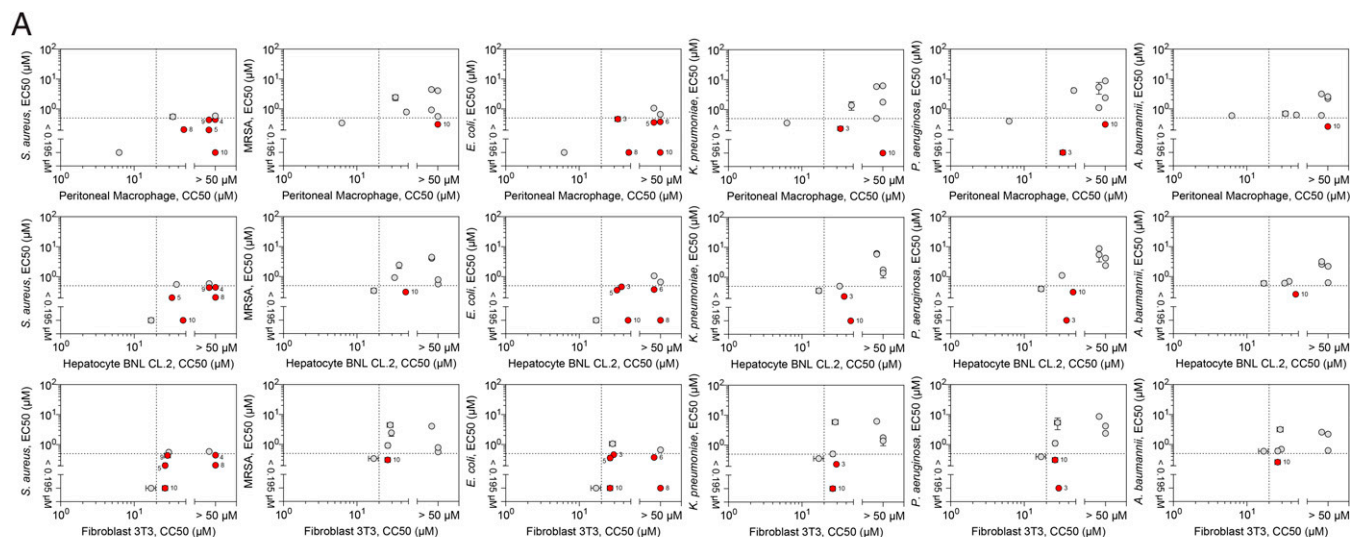
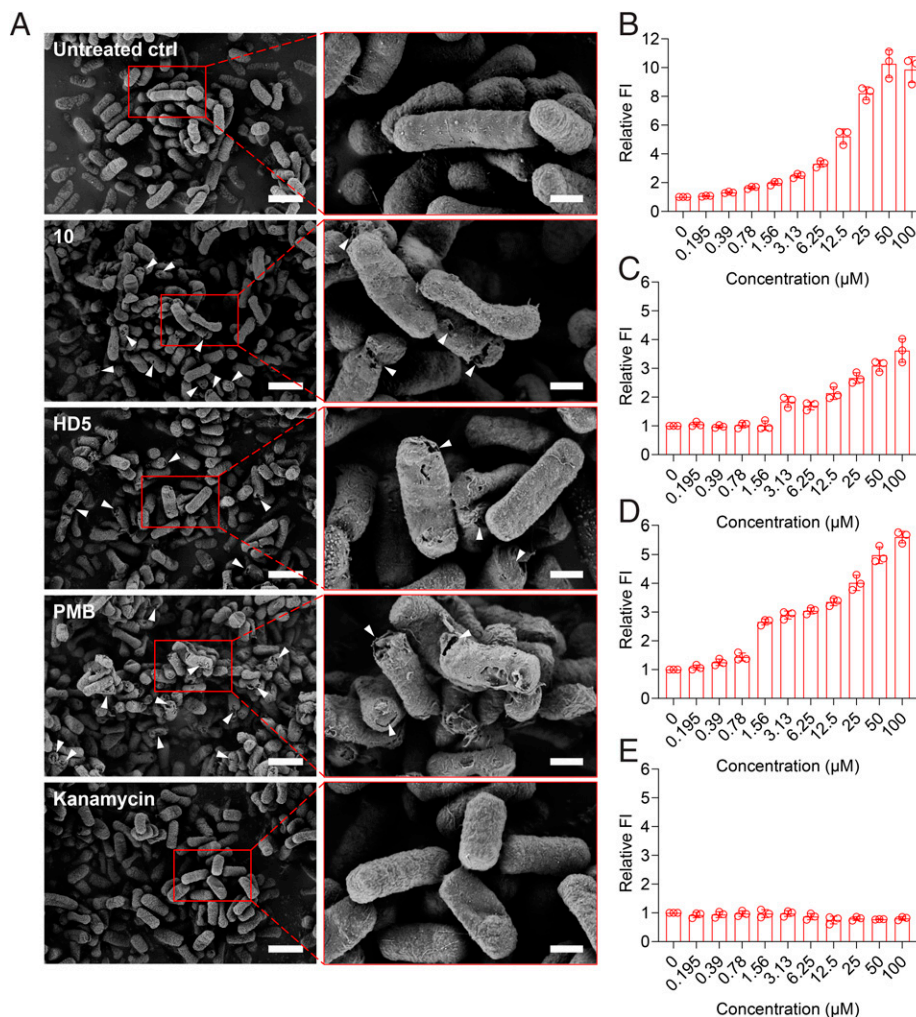**Fig. 3.** In vitro validation and SAR studies. (*A*) EC$_{50}$-CC$_{50}$ plots present the EC$_{50}$ values of peptidomimetic antibiotics against members of ESKAPE pathogens and the CC$_{50}$ values of peptidomimetic antibiotics to mammalian cells. Red points represent peptidomimetic antibiotics with a high therapeutic index. (*B*) In vitro antimicrobial activity of **5**, **10**, and Imipenem Cilastatin against clinically isolated bacteria. Data are presented as mean ± SD. The EC$_{50}$ values of the tested compounds are indicated for each pathogen, which are fitted by using a four-parameter dose–response model. All experiments were performed in triplicate.

(Fig. 5 *E* and *F*). However, OmpA periplasmic domain was not strongly bound by **10** and HD5, as indicated by their rapid dissociation (*SI Appendix*, Fig. S14).

We then investigated the OM permeability on OmpA-knockout *E. coli* (*E. coli*$^{\Delta OmpA}$). Results showed that the enhancement of OM permeability resulted from **10** challenge significantly decreased on *E. coli*$^{\Delta OmpA}$ as compared with wild-type *E. coli* (*E. coli*^{WT}) (Fig. 5*G*). Additionally, deleting OmpA from *E. coli* indeed attenuated the bactericidal activity of low-dose **10** with approximately twofold increasement in EC$_{50}$ (Fig. 5*H* and *SI Appendix*, Fig. S15*A*). These findings verified OmpA as one of the surface targets of **10**, in which the **10**-binding domain was the N-terminal β-barrel structure. Nevertheless, comparing bacterial cells with/without OmpA showed insignificant change in minimal bactericidal concentration (MBC) of **10** (*SI Appendix*, Fig. S15*B*), suggesting that **10** is likely to have a second, OmpA-independent MoA to disrupt OM.

Thus, we next tested if **10** also targeted LPS similarly to other CAMPs' membrane activity. Adding purified LPS potently antagonized bactericidal activity of **10** in a concentration-dependent manner (*SI Appendix*, Fig. S16*A*). This inhibitory effect to LPS was dramatic, as LPS at concentration of 25 μg/mL increased approximately sixfold the MBC of **10** and fourfold the MBC of PMB, but showed no effect on antimicrobial activity of kanamycin, suggesting LPS might be an important surface target of **10** (Fig. 5*I* and *SI Appendix*, Fig. S16). We further assessed the molecular interaction between **10** and LPS by a fluorescent quenching assay. LPS effectively quenched the fluorescence of compound **10** in a concentration-dependent manner with a high quenching constant (K_{SV}) (Fig. 5 *J* and *K*) that reported strong affinity between LPS and **10** (K_D ~0.793 nM) (Fig. 5 *J* and *K*). To test the ability of **10** to inactivate LPS, we performed a limulus amebocyte lysate assay that showed LPS was dose-proportionally neutralized by **10** (Fig. 5*L*). Structurally, LPS is composed of an

Luo et al.
Human defensin-inspired discovery of peptidomimetic antibiotics

PNAS | 5 of 11
https://doi.org/10.1073/pnas.2117283119

Fig. 4. Peptidomimetic antibiotic **10** exhibits membrane-perturbance activity to gram-negative OM. (*A*) Scanning electron microscopy of *E. coli* ATCC25922 untreated or incubated with different types of antimicrobials including **10**, HD5, PMB, and kanamycin. (Scale bars, *Left*, 2 μm.) Red frames highlight the high-magnification fields. (Scale bars, 500 nm.) (*B–E*) OM permeability of *E. coli* ATCC25922 probed with NPN after treating with different anti-microbials including **10** (*B*), HD5 (*C*), PMB (*D*), and kanamycin (*E*) for 1 h. Permeability of OM is positively corelated with the fluorescent intensity (FI) generated from NPN. The fluorescence data of NPN were normalized to relative FI. Data are presented as mean ± SD. All experiments were performed in triplicate.

O-antigen, a core polysaccharide, and a lipid A domain, in which lipid A represents the toxic core of LPS and usually is the binding domain of LPS-targeting antibiotics (e.g., PMB) (31, 32). Consequently, we next examined whether **10** neutralizes LPS through acting on lipid A domain. It is reported that divalent ions (e.g., Mg^{2+}) can bridge and neutralize the negatively charged lipid A domain in LPS by electrostatic interaction, thereby contributing to tight packing and low permeability (33, 34). NPN fluorescent probe assay demonstrated that incorporation of Mg^{2+} indeed protected the integrity of *E. coli* OM from the attack of **10** (Fig. 5*M*). We thus investigated the effect of Mg^{2+} on the bactericidal activity of compound **10**. As expected, incorporation of Mg^{2+} significantly diminished **10**'s activity with fourfold increase of MBC (Fig. 5 *N* and *O*). These results revealed that both LPS and OmpA were targets for **10** to exert membrane activity.

In summary, our defensin-inspired antibiotic **10** perfectly preserved the membrane activity of its parent HD5, with a similar MoA of targeting the OmpA β-barrel domain and LPS lipid A domain.

Bacterial 70S Ribosome Is a Potential Intracellular Target of Peptidomimetic Antibiotic 10. Although we uncovered the MoA of membrane activity, we found the RNA-sequencing (RNA-seq)

profile of *E. coli* treated by **10** was significantly different from that of HD5 and PMB (*SI Appendix*, Fig. S17). Hence, we asked if there might be another distinct MoA contributing to **10**'s antimicrobial action, in addition to membrane perturbation. Kyoto Encyclopedia of Genes and Genomes (KEGG) enrichment analysis revealed that treatment by **10** led to large up-regulation of numerous genes encoding 70S ribosomal subunits that all were enriched in the ribosome pathway (Fig. 6 *A* and *B*). Such an enrichment map was also distinct from that of HD5 and PMB (Fig. 6*B* and *SI Appendix*, Fig. S18). Considering that bacterial ribosome has already been identified as a mature and highly druggable target for antibiotics (e.g., kanamycin) (35), we rationally speculated 70S ribosome might be an independent intracellular target of **10**. To verify this, we performed an antimicrobial block assay to test if exogenous *E. coli* 70S ribosome could block the bactericidal effect of compound **10**. Surprisingly, incorporating *E. coli* 70S ribosome largely inhibited the activity of **10** at an extremely low concentration, with approximately eightfold enhancement of MBC value, this inhibitory action was stronger than that of LPS and OmpA (Fig. 6*C* and *SI Appendix*, Fig. S19*A*). As expected, we found *E. coli* 70S ribosome antagonized kanamycin but failed to affect activity of PMB (Fig. 6*C* and *SI Appendix*, Fig. S19 *B* and *C*). To investigate in-depth
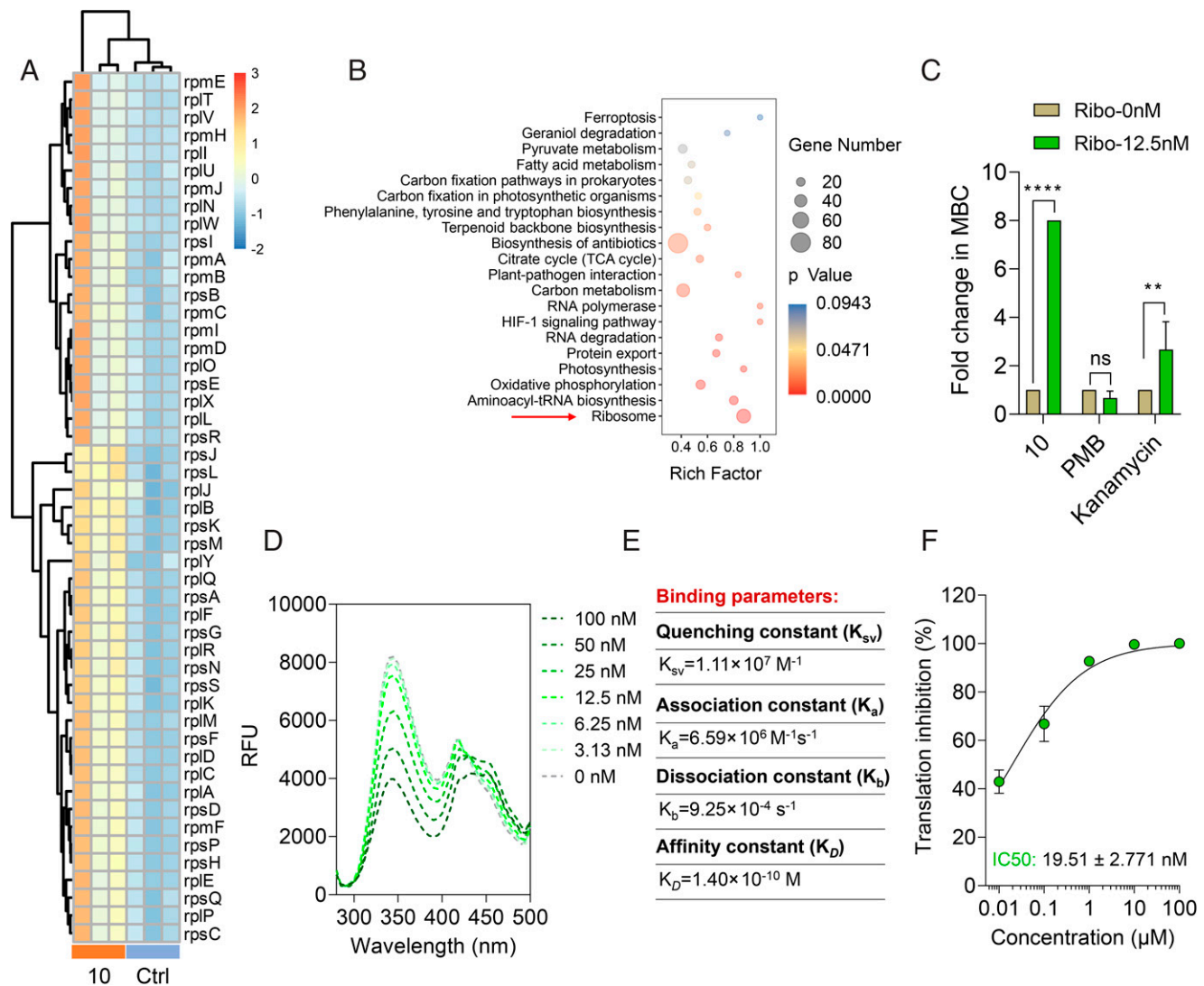
molecular interaction between **10** and *E. coli* 70S ribosome, we performed a fluorescent quenching assay. Results showed 70S ribosome also dramatically quenched the fluorescence of **10** in a concentration-dependent manner, with a $K_{sv} \sim 1.11 \times 10^7$ M^{-1} that improved ~30-fold compared with that of LPS (Fig. 6 *D* and *E*). In addition, **10** also showed stronger affinity to 70S ribosome
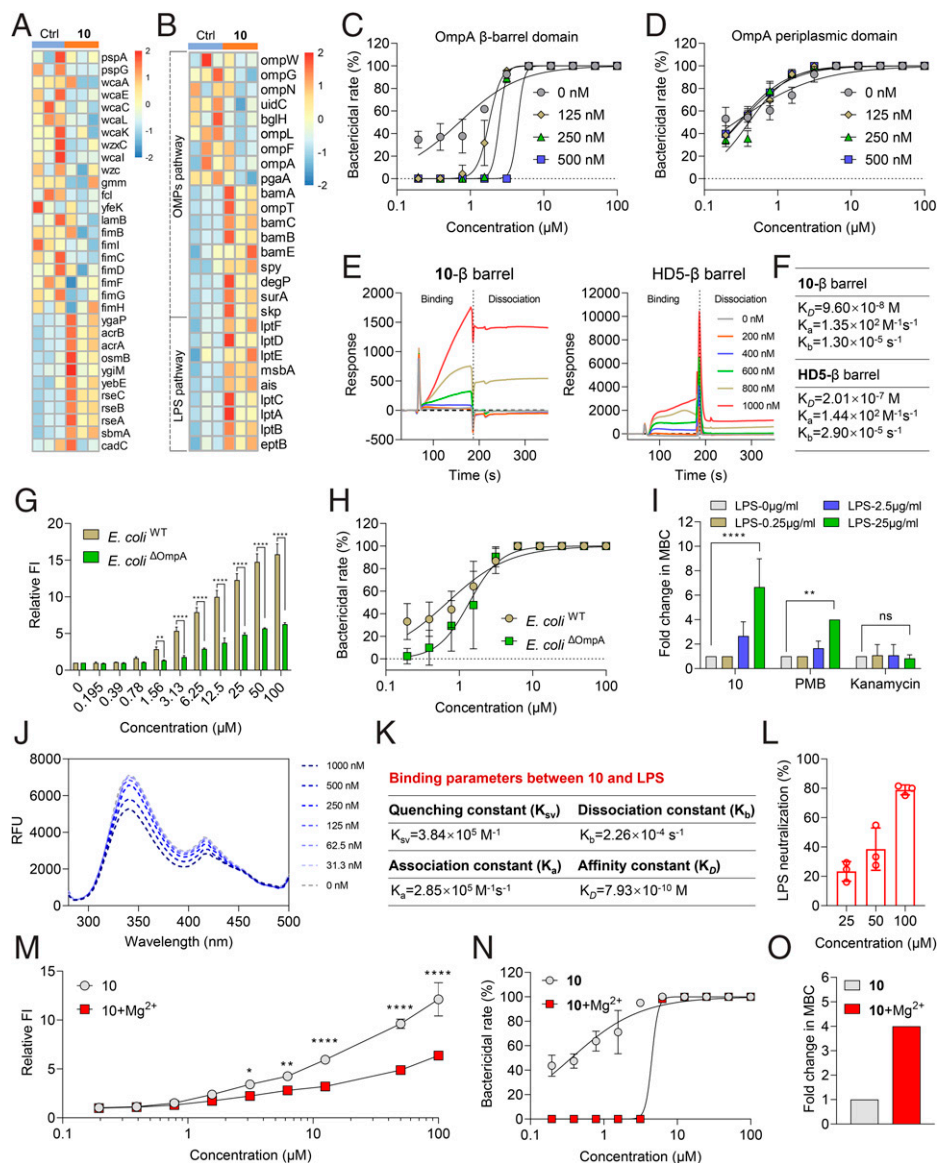
Fig. 5. Peptidomimetic antibiotic **10** exerts membrane activity by targeting OmpA and LPS. (*A*) RNA-seq profile showing the alterations of bacterial envelope stress-related genes in *E. coli* treated with **10**; data are presented using heatmap, each group was repeated in triplicate. (*B*) RNA-seq profile uncovering the significant alterations of genes related to OMPs pathway and LPS pathway, data are presented using heatmap, each group was repeated in triplicate. (*C*) In vitro bactericidal activity of **10** against *E. coli* in presence of different concentrations of recombinant OmpA β-barrel domain. Addition of OmpA β-barrel domain antagonized activity of low-concentration **10** in a concentration-dependent manner. Data are mean ± SD with triplicate experiments. (*D*) In vitro bactericidal activity of **10** against *E. coli* in the presence of different concentrations of recombinant OmpA periplasmic domain. Addition of OmpA periplasmic domain did not affect activity of low-concentration **10**. Data are mean ± SD with triplicate experiments. (*E*) SPR analysis of interaction between **10**/HD5 and OmpA β-barrel domain. (*F*) Table recording the interactive parameters calculated from SPR assay, including the equilibrium dissociation constant (K_D), association constant (K_a), and dissociation constant (K_b). (*G*) OM permeability of wild-type *E. coli* (*E. coli*^{WT}) and OmpA-deficient *E. coli* (*E. coli*$^{\Delta OmpA}$) probed with NPN, after treating with **10** for 1 h. Permeability of OM is positively corelated with the FI generated from NPN. The fluorescence data of NPN were normalized to relative FI. (*H*) In vitro bactericidal activity of **10** against wild-type *E. coli* (*E. coli*^{WT}) and OmpA-deficient *E. coli* (*E. coli*$^{\Delta OmpA}$), the experiments were repeated nine times. (*I*) In vitro virtual-colony count assay determining fold-change in MBCs of **10**, PMB, and kanamycin against *E. coli* in the presence of different concentrations of LPS. Addition of LPS significantly improved the MBCs of **10** and PMB, but not kanamycin's MBC. (*J*) Fluorescent quenching analysis of interaction between **10** and LPS. Fluorescent intensities of **10** were significantly quenched by adding LPS in a concentration-dependent manner. Experiments were repeated in triplicate. (*K*) Table recording the binding parameters calculated from fluorescent quenching assay, including the quenching constant (K_{SV}), association constant (K_a), dissociation constant (K_b), and equilibrium dissociation constant (K_D). (*L*) Limulus amebocyte lysate assay detection of LPS neutralization of compound **10**. (*M*) OM permeability of *E. coli* probed with NPN, after treating with **10** in absence or presence of Mg^{2+} (50 μg/mL) for 1 h. Permeability of the OM is positively corelated with the FI generated from NPN. The fluorescence data of NPN were normalized to relative FI. (*N*) In vitro bactericidal activity of **10** against *E. coli* in the absence or presence of Mg^{2+} (50 μg/mL). (*O*) Fold-change in MBC of **10** against *E. coli* in the absence or presence of Mg^{2+} (50 μg/mL). Data are mean ± SD with triplicate experiments. Statistical significance was calculated by one/two-way analysis of variance with the Bonferroni correction for multiple comparisons. *$P < 0.05$, **$P < 0.01$, ***$P < 0.001$, ****$P < 0.0001$; ns, not significant.

Luo et al.
Human defensin-inspired discovery of peptidomimetic antibiotics

PNAS | 7 of 11
https://doi.org/10.1073/pnas.2117283119

Fig. 6. Peptidomimetic antibiotic **10** targets bacterial 70S ribosome and inhibits protein synthesis. (*A*) RNA-seq profile showing the alterations of genes encoding ribosomal subunits in *E. coli* treated with **10**, data are presented using heatmap, each group was repeated in triplicate. (*B*) KEGG enrichment analysis of differentially expressed genes of RNA-seq profile in *E. coli* treated with **10**. (*C*) In vitro virtual-colony count assay determining fold change in MBCs of **10**, PMB and kanamycin against *E. coli* in presence of *E. coli* 70S ribosome. Addition of 70S ribosome significantly improved the MBCs of **10** and kanamycin, but not PMB's MBC. Data are mean ± SD with triplicate experiments. **$P < 0.01$, ****$P < 0.0001$; ns, not significant. (*D*) Fluorescent quenching analysis of interaction between **10** and *E. coli* 70S ribosome. FIs of **10** were significantly quenched by adding 70S ribosome in a concentration-dependent manner. (*E*) Table recording the binding parameters calculated from fluorescent quenching assay, including the quenching constant (K_{SV}), association constant (K_a), dissociation constant (K_b), and equilibrium dissociation constant (K_D). (*F*) In vitro translation assay demonstrating the inhibition of protein synthesis ability of 70S ribosome with the treatment of **10**. Data are mean ± SD with triplicate experiments. Statistical significance was calculated by one/two-way analysis of variance with the Bonferroni correction for multiple comparisons.

than that of LPS (K_D ~0.140 nM) (Fig. 6*E*). Additional in vitro translation assay proved compound **10** was able to potently inhibit protein synthesis of *E. coli* 70S ribosome, with a nanomolar IC$_{50}$ (~19.51 ± 2.771 nM) (Fig. 6*F*). Collectively, these findings implicated bacterial 70S ribosome as a potential intracellular target of compound **10** that might confer the antimicrobial activity by impairing protein synthesis.

In Vivo Biological Profiles. To assess the in vivo therapeutic performance of **10**, animal models of sepsis and bacterial pneumonia were established. In *E. coli*-septic mice, untreated controls all died within 12 h, while administration of **10** manifested therapeutic efficacy comparable to the last-resort antibiotic PMB (Fig. 7*A*). Compound **10** considerably decreased the bacterial burden in the blood and organs (Fig. 7 *B* and *C*)

and, consequently, attenuated multiorgan injury (*SI Appendix*, Fig. S20). Mice with *K. pneumoniae*-induced pneumonia displayed high mortality with 100% lethality within 48 h. Treatment with **10** resulted in an 80% survival rate; PMB treatment resulted in a 100% survival rate (*SI Appendix*, Fig. S21*A*) but PMB was ineffective in *S. aureus*-induced pneumonia (*SI Appendix*, Fig. S21*B*), where **10** showed 100% survival rates comparable to vancomycin (*SI Appendix*, Fig. S21*B*). As expected, the bacterial burden in bronchoalveolar lavage fluid was in keeping with the results of survival rates (*SI Appendix*, Fig. S21 *C* and *D*). The total cell count and protein concentration in bronchoalveolar lavage fluid were also significantly reduced in animals treated with **10** (*SI Appendix*, Fig. S21 *E* and *F*), indicating decreased damage to pulmonary barriers.
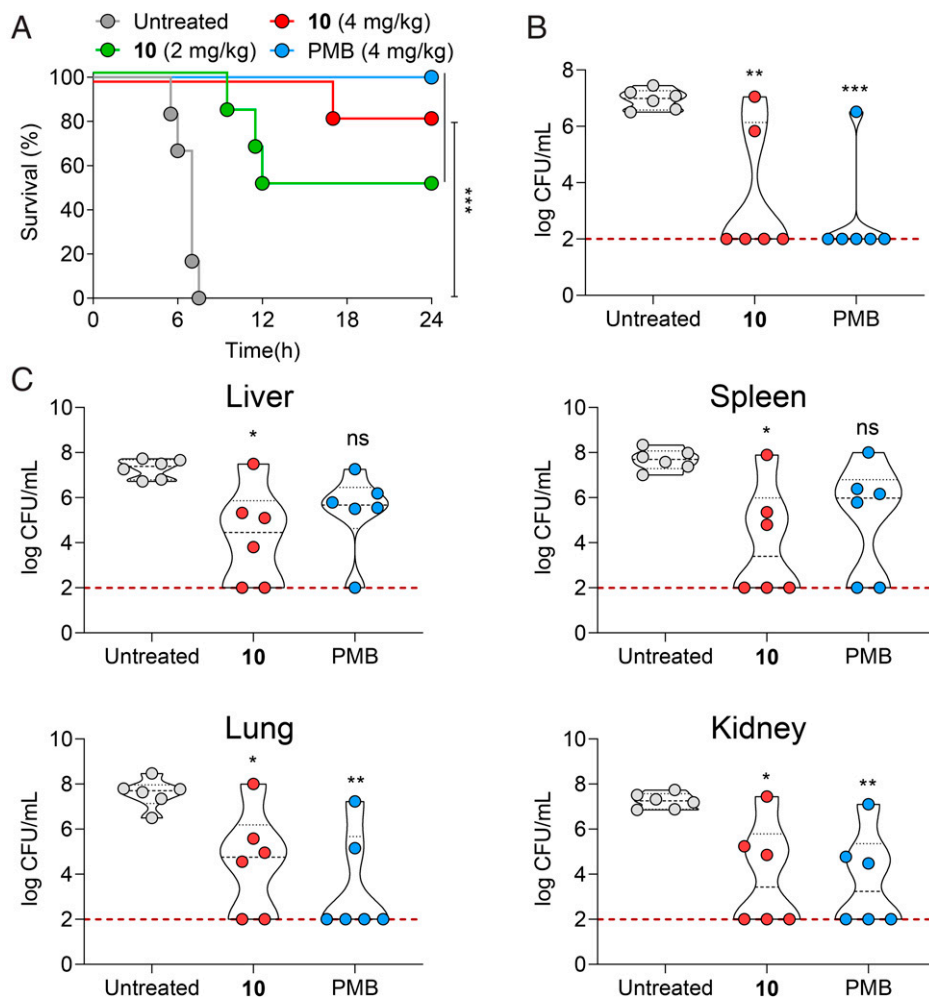
Fig. 7. Protection of mice against *E. coli*-challenged septicemia. (*A*) Kaplan–Meier percent survival analysis of C57BL/6 mice challenged with *E. coli* and concomitantly treated with compound **10** or PMB. *n* = 6 per group. (*B*) Determination of bacterial burden in blood from *E. coli*-challenged mice with/without treatment of compound **10** or PMB. *n* = 6 per group. Dashed line indicates the limit of detection. (*C*) Determination of bacterial burden in organs, including liver, spleen, lung, and kidney, from *E. coli*-challenged mice with/without treatment of compound **10** or PMB. *n* = 6 per group. Dashed line indicates the limit of detection. Statistical significance was calculated by one-way analysis of variance with the Bonferroni correction for multiple comparisons. *$P < 0.05$, **$P < 0.01$, ***$P < 0.001$; ns, not significant.

To assess the in vivo safety of **10**, healthy C57BL/6 mice were intraperitoneally injected with high doses of **10**. Mice showed 100% survival after challenges with extremely high doses of 64, 128, and 264 mg/kg of **10** (*SI Appendix*, Fig. S22A), suggesting its pharmacologically acceptable safety profile. We then evaluated the in vivo stability through a single-dose pharmacokinetic study. Injection of **10** generated a peak plasma concentration of 3,455 ng/mL and a half-life of 2.35 h (*SI Appendix*, Fig. S22B), indicating a favorable in vivo stability.

Discussion

Resistance to antimicrobials is an increasing threat to global healthcare due to the emergence of drug resistance and limited development of new antibiotics (1, 3, 5). Valuable new antibiotics now include highly drug-like peptide antimicrobials (e.g., teixobactin and darobactin) from bacterial resources based on biosynthetic gene clusters (28, 36, 37). Application of artificial intelligence methods has advanced antibiotic discovery, as exemplified by introducing known compounds used in other fields as antibiotics through deep learning (38). Incorporating modular design and chimeric chemistry can transform "old" antibiotics to "new" antibiotics, thereby mitigating antimicrobial resistance (39, 40). Despite these significant advances, the huge demand for novel antibiotics necessitates continuous discovery/design of alternatives. A potential resource is the antimicrobial chemistry of human endogenous antibiotics, such as HD5 (6, 17), as these CAMPs often contain regions of cationicity and hydrophobicity (e.g., amphiphilicity) segregated in a stable structure and are thought to kill bacteria by primarily targeting their negatively charged membrane, thus being less likely to induce antibiotic resistance (6, 41). However, intrinsic shortcomings of CAMPs, such as susceptibility to proteolysis, inadequate bactericidal activity, and difficult chemical synthesis and modification hinder direct translation to the clinic (6, 7, 41).

Several peptidomimetic strategies, such as foldamers and flavonoid-based mimics, have alleviated some of the intrinsic shortcomings of these CAMPs (7, 9, 11, 13). The "foldamers" approach incorporates different types of unnatural residues/moieties to restrict backbone flexibility, thus stabilizing specific conformations and enhancing metabolic stability (7–9). By fine-tuning the relative positions of cationic and hydrophobic residues on the peptide backbone, improved antimicrobial activity and enhanced selectivity could be achieved (42). This strategy led to the design of magainin foldamers, such as helical peptoid mimics and rationally stapled magainin II (10–12). Similarly, the small-molecule–based approach mainly considers the factors of

Luo et al.
Human defensin-inspired discovery of peptidomimetic antibiotics

PNAS | 9 of 11
https://doi.org/10.1073/pnas.2117283119

scaffold rigidity, cationicity, and hydrophilicity, as exemplified by rigid and hydrophobic flavonoids decorated with cationic groups (13–15). Of note, although unnatural peptides comprising β-amino acids (i.e., β-peptides) are resistant to proteolysis (8, 43, 44), they do not mimic helical conformations adopted by some parent CAMPs (44, 45), in contrast to α/β-peptides that contain both α- and β-residues (44, 46). Srinivas et al. (16) introduced a rigid β-turn, D-Pro-L-Pro, to mimic the β-hairpin structure of protegrin I, and significantly improved peptide stability. The resultant product Murepavadin and its inhaled formulation entered clinical trials for the treatment of *P. aeruginosa* pneumonia (5, 16).

Structural classes of antimicrobial peptides include highly disordered linear peptides that adopt an α-helical structure upon membrane binding (e.g., magainin), β-hairpin peptides stabilized by two intramolecular disulfides (e.g., protegrins), and mammalian defensins that fold into a three-stranded β-sheet conformation stabilized by three intramolecular disulfide bridges (17, 47). Compared with defensins, magainin, and protegrins are relatively simple at the structural level and their peptidomimetic strategies are understandably focused on localized modifications to improve backbone rigidity and, thus, proteolytic stability and to modulate amphiphilicity for enhanced bioactivity and reduced cytotoxicity (7, 13, 42). By contrast, human α-defensins are only moderately cationic and, in fact, cationicity is not the most important functional determinant for their functions (48).

Furthermore, while human α-defensins kill gram-negative bacteria through membrane disruption in a largely structure-independent fashion, they kill gram-positive strains by sequestering lipid II to inhibit bacterial cell wall synthesis (24, 49), which is structure-dependent. Extensive mutational studies of the prototypic human α-defensin HNP1 and HD5 elucidated hydrophobic residues at the C terminus, selective Arg residues, disulfide-bonding and dimerization as functionally critical elements (50–53). In particular, hydrophobicity and the ability of human α-defensins to dimerize, oligomerize, and multimerize upon target binding are thought to be an overriding determinant for their functional pleiotropism (54), as exemplified by a multiplicity of molecular targets of α-defensins, including lipids and microbial membranes, bacterial cell wall components, bacterial toxins and virulence factors, viral proteins, carbohydrates and glycoproteins, cellular receptors and host proteins, and nucleic acids (48). In light of the substantive differences between defensins and other classes of CAMPs at the structural, functional, and mechanistic levels, we chose a global peptidomimetic strategy, where structure-guided molecular dissection of defensin-target interactions allowed us to make novel contributions to the fertile field of rationally designed antibiotic mimics.

Inspired by the pharmacophore concept in small-molecule drug design (55, 56), we mapped the interactions between HD5 and its potential targets using computational chemistry approaches to identify key pharmacophore fragments in HD5, resulting in the simple tetra-peptide scaffold R^{25}-L^{26}-Y^{27}-R^{28} for functionalization and optimization. In contrast to foldamers and flavonoid-based mimics whose backbones are rigidified, our core scaffold is flexible to ensue adaptive conformations for specific and high-affinity molecular interactions. Since hydrophobicity dominates α-defensin functionality, we reasoned that terminal modification of the scaffold by nonpolar moieties, such as long alkyl chains and aromatic groups, would not only enhance peptide killing of bacteria in general, but also modulate its selectivity toward gram-positive and gram-negative bacteria and possibly its cytotoxicity profile as well. This approach was validated by our in vitro SAR and in vivo efficacy studies. Of note, terminal modifications of the tetra-peptide scaffold by hydrophobic moieties did not cause functionally adverse reduction in solubility and likely contributed to enhanced proteolytic

resistance and improved metabolic stability of peptide compounds, as verified by pharmacokinetic studies. Since the scaffold of compound **2** is sufficiently small, the addition of bulky structural elements may lead to a different class of compounds with significantly altered activity profiles and modes of action, an important lesson for the design of defensin-derived peptidomimetics. Our core scaffold may be a useful template for the design of other classes of peptidomimetic antibiotics as well.

Despite previous efforts in designing HD5 derivatives through residue substitution and nanotechnology (20, 57), their pharmacokinetic properties and efficacy in combatting high-risk CR-/PDR-clinical isolates have yet to be demonstrated. Of the newly designed antibiotics, **10** exhibited high activity and a wide therapeutic window. Importantly, **10** was also effective against a series of clinically isolated CR- and PDR-superbugs, against which the first-line antibiotic Imipenem Cilastatin is ineffective. Notably, the CR-*K. pneumoniae* and PDR-*P. rettgeri* were isolated from two intensive care unit patients, both of whom suffered bacterial infection-induced critical illnesses, such as multiorgan dysfunction syndrome and septic shock (for details, see *SI Appendix*, Tables S1 and S2). Our peptidomimetic antibiotics may offer a possibility to manage these critical conditions in the future. Compound **10** has a unique structure, consisting of an N-terminal p-aminobenzenesulfonyl group, a core peptide scaffold, and a palmityl chain. Despite its origin from HD5, **10** is quite different from the parent defensin in both biological activity profiles and MoAs. Additional studies are warranted to elucidate the molecular basis underlying the functional and mechanistic differences between **10** and HD5. It is conceivable that our concept for redesigning HD5 can be generalized into a standard protocol to guide redesign of other defensins from hits to lead compounds to drug candidates.

Against clinically "difficult-to-treat" pathogens, especially for gram-negative bacteria, multimodal antibiotics with double MoAs or multiple targets may avoid the high-frequency antimicrobial resistance/persistence manifested by evolving gram-negative bacteria (58, 59). Specifically, gram-negative bacteria possess a tight membrane barrier that contains a lipidic IM and an LPS-coated OM (60). Because of the existence of OM, compounds with hydrophobicity or a relatively large size (~ >600 Da) are hindered from entering bacterial cells (5). Hydrophilic compounds with low molecular weight can penetrate the OM; however, they are hindered by the lipidic IM (5). The double-membrane barrier equips gram-negative bacteria with a stronger tolerance to antimicrobials, and impedes the development of antibiotics against gram-negative bacteria (5). Our lead candidate, **10**, is a relatively large molecule with molecular mass of 1184.57 Da that is larger than the cutoff for compounds to penetrate the OM (~600 Da). Remarkably, **10** showed broad-panel activity against a series of gram-negative bacteria, including multidrug-resistant strains. We found that LPS and OmpA were the surface targets of **10** that mediated its membrane activity, and we also identified bacterial 70S ribosome as a potential intracellular target of **10**. The double mechanisms of membrane perturbation and inhibition of protein synthesis might synergistically contribute to the effective killing of **10** to gram-negative bacteria. Genetic knockout of OmpA could significantly attenuate the OM permeabilization caused by **10**, but it could not abolish **10**'s bactericidal activity, suggesting that single-target mutation may not generate antimicrobial resistance to **10**. Nevertheless, detailed structural basis of **10** in complex with its molecular targets remains unclear. Future refinement of the MoAs of **10** should facilitate the discovery, design, and evaluation of new classes of peptide antibiotics to confront the challenge of antimicrobial resistance. Finally, although we identified 70S ribosome as a potential target that warrants in-depth investigation in the future, the possibility of the existence of other molecular targets responsible for the antibacterial action of **10** cannot be formally excluded.

1. R. Laxminarayan *et al.*, Antibiotic resistance-the need for global solutions. *Lancet Infect. Dis.* **13**, 1057–1098 (2013).
2. J. O'Neill *Tackling Drug-Resistant Infections Globally: Final Report and Recommendations* (The Review on Microbial Resistance, Wellcome Trust, 2016).
3. R. Laxminarayan *et al.*, Access to effective antimicrobials: A worldwide challenge. *Lancet* **387**, 168–175 (2016).
4. WHO, *Global Priority List of Antibiotic-resistant Bacteria to Guide Research, Discovery, and Development of New Antibiotics* (World Health Organization, 2017).
5. K. Lewis, The science of antibiotic discovery. *Cell* **181**, 29–45 (2020).
6. N. Mookherjee, M. A. Anderson, H. P. Haagsman, D. J. Davidson, Antimicrobial host defence peptides: Functions and clinical potential. *Nat. Rev. Drug Discov.* **19**, 311–332 (2020).
7. J. S. Laursen, J. Engel-Andreasen, C. A. Olsen, β-Peptoid foldamers at last. *Acc. Chem. Res.* **48**, 2696–2704 (2015).
8. W. S. Horne, S. H. Gellman, Foldamers with heterogeneous backbones. *Acc. Chem. Res.* **41**, 1399–1408 (2008).
9. H. Yokoo, M. Hirano, T. Misawa, Y. Demizu, Helical antimicrobial peptide foldamers containing non-proteinogenic amino acids. *ChemMedChem* **16**, 1226–1233 (2021).
10. J. A. Patch, A. E. Barron, Helical peptoid mimics of magainin-2 amide. *J. Am. Chem. Soc.* **125**, 12092–12093 (2003).
11. M. A. Schmitt, B. Weisblum, S. H. Gellman, Unexpected relationships between structure and function in α,β-peptides: Antimicrobial foldamers with heterogeneous backbones. *J. Am. Chem. Soc.* **126**, 6848–6849 (2004).
12. R. Mourtada, Design of stapled antimicrobial peptides that are stable, nontoxic and kill antibiotic-resistant bacteria in mice. *Nat. Biotechnol.* **37**, 1186–1197 (2019).
13. S. Lin, J. D. Wade, S. Liu, De novo design of flavonoid-based mimetics of cationic antimicrobial peptides: Discovery, development, and applications. *Acc. Chem. Res.* **54**, 104–119 (2021).
14. J. J. Koh *et al.*, Nonpeptidic amphiphilic xanthone derivatives: Structure-activity relationship and membrane-targeting properties. *J. Med. Chem.* **59**, 171–193 (2016).
15. Y. Chen *et al.*, Synthesis and biological evaluation of indole-based peptidomimetics as antibacterial agents against Gram-positive bacteria. *Eur. J. Med. Chem.* **226**, 113813 (2021).
16. N. Srinivas *et al.*, Peptidomimetic antibiotics target outer-membrane biogenesis in *Pseudomonas aeruginosa*. *Science* **327**, 1010–1013 (2010).
17. T. Ganz, Defensins: Antimicrobial peptides of innate immunity. *Nat. Rev. Immunol.* **3**, 710–720 (2003).
18. N. H. Salzman, D. Ghosh, K. M. Huttner, Y. Paterson, C. L. Bevins, Protection against enteric salmonellosis in transgenic mice expressing a human intestinal defensin. *Nature* **422**, 522–526 (2003).
19. H. R. Chileveru *et al.*, Visualizing attack of *Escherichia coli* by the antimicrobial peptide human defensin 5. *Biochemistry* **54**, 1767–1777 (2015).
20. R. Lei *et al.*, Self-assembling myristoylated human α-defensin 5 as a next-generation nanobiotics potentiates therapeutic efficacy in bacterial infection. *ACS Nano* **12**, 5284–5296 (2018).
21. E. Kudryashova *et al.*, Human defensins facilitate local unfolding of thermodynamically unstable regions of bacterial protein toxins. *Immunity* **41**, 709–721 (2014).
22. C. Wang *et al.*, A simplified derivative of human defensin 5 with potent and efficient activity against multidrug-resistant *Acinetobacter baumannii*. *Antimicrob. Agents Chemother.* **62**, e01504–e01517 (2018).
23. K. M. Varney *et al.*, Turning defense into offense: Defensin mimetics as novel antibiotics targeting lipid II. *PLoS Pathog.* **9**, e1003732 (2013).
24. E. de Leeuw *et al.*, Functional interaction of human neutrophil peptide-1 with the cell wall precursor lipid II. *FEBS Lett.* **584**, 1543–1548 (2010).
25. T. Awang, P. Pongprayoon, The adsorption of human defensin 5 on bacterial membranes: Simulation studies. *J. Mol. Model.* **24**, 273 (2018).
26. S. W. Jung, J. Lee, A. E. Cho, Elucidating the bacterial membrane disruption mechanism of human alpha-defensin 5: A theoretical study. *J. Phys. Chem. B* **121**, 741–748 (2017).
27. P. A. Smith *et al.*, Optimized arylomycins are a new class of Gram-negative antibiotics. *Nature* **561**, 189–194 (2018).
28. Y. Imai *et al.*, A new antibiotic selectively kills Gram-negative pathogens. *Nature* **576**, 459–464 (2019).
29. S. G. Smith, V. Mahon, M. A. Lambert, R. P. Fagan, A molecular Swiss army knife: OmpA structure, function and expression. *FEMS Microbiol. Lett.* **273**, 1–11 (2007).
30. H. Ishida, A. Garcia-Herrero, H. J. Vogel, The periplasmic domain of *Escherichia coli* outer membrane protein A can undergo a localized temperature dependent structural transition. *Biochim. Biophys. Acta* **1838**, 3014–3024 (2014).
31. D. R. Storm, K. S. Rosenthal, P. E. Swanson, R. Daniel, Polymyxin and related peptide antibiotics. *Annu. Rev. Biochem.* **46**, 723–763 (1977).
32. T. W. Cullen *et al.*, Gut microbiota. Antimicrobial peptide resistance mediates resilience of prominent gut commensals during inflammation. *Science* **347**, 170–175 (2015).
33. C. R. Raetz, C. Whitfield, Lipopolysaccharide endotoxins. *Annu. Rev. Biochem.* **71**, 635–700 (2002).
34. M. Song *et al.*, A broad-spectrum antibiotic adjuvant reverses multidrug-resistant Gram-negative pathogens. *Nat. Microbiol.* **5**, 1040–1050 (2020).
35. D. N. Wilson, Ribosome-targeting antibiotics and mechanisms of bacterial resistance. *Nat. Rev. Microbiol.* **12**, 35–48 (2014).
36. L. L. Ling *et al.*, A new antibiotic kills pathogens without detectable resistance. *Nature* **517**, 455–459 (2015).
37. E. J. Culp *et al.*, Evolution-guided discovery of antibiotics that inhibit peptidoglycan remodelling. *Nature* **578**, 582–587 (2020).
38. J. M. Stokes *et al.*, A deep learning approach to antibiotic discovery. *Cell* **180**, 688–702 (2020).
39. A. Luther *et al.*, Chimeric peptidomimetic antibiotics against Gram-negative bacteria. *Nature* **576**, 452–458 (2019).
40. Q. Li *et al.*, Synthetic group A streptogramin antibiotics that overcome Vat resistance. *Nature* **586**, 145–150 (2020).
41. B. P. Lazzaro, M. Zasloff, J. Rolff, Antimicrobial peptides: Application informed by evolution. *Science* **368**, eaau5480 (2020).
42. G. N. Tew, R. W. Scott, M. L. Klein, W. F. Degrado, De novo design of antimicrobial polymers, foldamers, and small molecules: From discovery to practical applications. *Acc. Chem. Res.* **43**, 30–39 (2010).
43. T. Hintermann, D. Seebach, The biological stability of β-peptides: No interactions between α- and β-peptidic structures? *Chimia (Aarau)* **51**, 244–247 (1997).
44. J. W. Checco, S. H. Gellman, Targeting recognition surfaces on natural proteins with peptidic foldamers. *Curr. Opin. Struct. Biol.* **39**, 96–105 (2016).
45. J. D. Sadowsky *et al.*, (α/β+α)-peptide antagonists of BH3 domain/Bcl-x(L) recognition: Toward general strategies for foldamer-based inhibition of protein-protein interactions. *J. Am. Chem. Soc.* **129**, 139–154 (2007).
46. L. M. Johnson, S. H. Gellman, α-Helix mimicry with α/β-peptides. *Methods Enzymol.* **523**, 407–429 (2013).
47. M. Zasloff, Antimicrobial peptides of multicellular organisms. *Nature* **415**, 389–395 (2002).
48. R. I. Lehrer, W. Lu, α-Defensins in human innate immunity. *Immunol. Rev.* **245**, 84–112 (2012).
49. T. Schneider *et al.*, Plectasin, a fungal defensin, targets the bacterial cell wall precursor Lipid II. *Science* **328**, 1168–1172 (2010).
50. G. Wei *et al.*, Through the looking glass, mechanistic insights from enantiomeric human defensins. *J. Biol. Chem.* **284**, 29180–29192 (2009).
51. G. Wei *et al.*, Trp-26 imparts functional versatility to human alpha-defensin HNP1. *J. Biol. Chem.* **285**, 16275–16285 (2010).
52. D. Xu *et al.*, Human enteric α-defensin 5 promotes shigella infection by enhancing bacterial adhesion and invasion. *Immunity* **48**, 1233–1244.e6 (2018).
53. M. Rajabi *et al.*, Functional determinants of human enteric α-defensin HD5: Crucial role for hydrophobicity at dimer interface. *J. Biol. Chem.* **287**, 21615–21627 (2012).
54. L. Zhao, W. Lu, Defensins in innate immunity. *Curr. Opin. Hematol.* **21**, 37–42 (2014).
55. C. Chang, S. Ekins, P. Bahadduri, P. W. Swaan, Pharmacophore-based discovery of ligands for drug transporters. *Adv. Drug Deliv. Rev.* **58**, 1431–1450 (2006).
56. S. Wang, G. Dong, C. Sheng, Structural simplification: An efficient strategy in lead optimization. *Acta Pharm. Sin. B* **9**, 880–901 (2019).
57. C. Wang *et al.*, Design of a potent antibiotic peptide based on the active region of human defensin 5. *J. Med. Chem.* **58**, 3083–3093 (2015).
58. D. J. Payne, M. N. Gwynn, , 5 D. J. Holmes, D. L. Pompliano, Drugs for bad bugs: Confronting the challenges of antibacterial discovery. *Nat. Rev. Drug Discov.* **6**, 29–40 (2007).
59. J. K. Martin, 2nd *et al.*, A dual-mechanism antibiotic kills Gram-negative bacteria and avoids drug resistance. *Cell* **181**, 1518–1532 (2020).
60. M. C. Sousa, New antibiotics target bacterial envelope. *Nature* **576**, 389–390 (2019).

Luo et al.
Human defensin-inspired discovery of peptidomimetic antibiotics

PNAS | 11 of 11
https://doi.org/10.1073/pnas.2117283119